Journal of Thermal Analysis, Vol. 34 (1988) 1427–1440

THERMAL ANALYSIS AND KINETICS OF OXIDATION OF MOLYBDENUM SULFIDES

Y. Shigegaki, S. K. Basu, M. Wakihara and *M. Taniguchi*

DEPARTMENT OF CHEMICAL ENGINEERING, TOKYO INSTITUTE OF TECHNOLOGY, O-OKAYAMA, MEGURO-KU, TOKYO-152, JAPAN

(Received December 10, 1987)

The thermal oxidation process of stoichiometric MoS_2 and nonstoichiometric "Mo_2S_3", together with the kinetics of oxidation of MoS_2, were studied by using TG and DTA techniques in the Po_2 range 1–0.0890 atm. MoS_2 was oxidized completely to MoO_3 in one step:

$$MoS_2 + 7/2\,O_2 \rightarrow MoO_3 + 2\,SO_2$$

Irrespective of Po_2 and the heating rate, "Mo_2S_3" was oxidized finally to MoO_3, via the following four steps:

$$\text{“}Mo_2S_3\text{”} \xrightarrow{\text{I}} \gamma\text{-}Mo_4O_{11(sur)} + \text{“}Mo_2S_3\text{”} \xrightarrow{\text{II}}$$

$$MoO_{2(sur)} + \text{“}Mo_2S_3\text{”} \xrightarrow{\text{III}} MoO_2 \xrightarrow{\text{IV}} MoO_3$$

where (sur) refers to the surface layer.

The kinetic study revealed that the oxidation (α = 0.01–0.90) of MoS_2 to MoO_3 was controlled by the kinetics

$$1-(1-\alpha)^{1/3} = kt$$

and that the apparent activation energies determined with the isothermal and the nonisothermal (10 deg min^{-1}) method were 98.1 ± 2.2 and 93.5 ± 3.0 kJ mol^{-1}, respectively, over the temperature range 540–625° and the Po_2 range 0.612–0.129 atm. The relationship between the rate constant k and Po_2 was determined.

In the Mo–S system, the hexagonal 2H–MoS_2, the monoclinic "Mo_2S_3" and metallic Mo can be obtained in solid-gas equilibrium reactions at temperatures higher than 610° [1–3]. In recent years, MoS_2 has been the subject of much interest as a lubricant for rotating and sliding components [4].

The oxidation and the kinetics of oxidation of MoS_2 are generally studied from the point of view of recovering molybdenum from molybdenite concentrate (ca. 90% MoS_2). Ong [5] reported an investigation on the oxidation of molybdenite compressed into pellets over the temperature range 360–461°. He suggested that the

John Wiley & Sons, Limited, Chichester
Akadémiai Kiadó, Budapest

oxidation occurs in stages, with MoO_2 as an intermediate. Other investigators [6–9] found this sequence in molybdenite oxidation until the sulfur has largely been removed from the solid phase. Wilkomirsky et al. [10] and Doheim et al. [11] reported the oxidation process to be

$$MoS_2 + 7/2\,O_2 \rightarrow MoO_3 + 2\,SO_2 \qquad (5)$$

The surface oxidation of pure MoS_2 (99%) was described by Ross et al. [12]. They found the formation of a monolayer of MoO_3 on the sulfide particles at 110°.

Although there are a large number of reports on the oxidation process and kinetics of molybdenite oxidation, there is considerable discrepancy between the published results (Table 1). On the other hand, no report has so far been published on pure MoS_2 or on "Mo_2S_3". The purpose of the present paper was to investigate the oxidation kinetics of MoS_2 and the oxidation processes of "Mo_2S_3" by using TG and DTA.

Table 1 Literature values of E for the oxidation of molybdenite

E, kJ mol^{-1}	Temp. range, °C	P_{O_2} range, atm	Method	Ref.
57.5	570–580	—	following SO_2	6
130.6	430–629	0.150–0.350	following SO_2	11
148.2	525–635	0.050–0.200	following SO_2	13
176.4	492–670	0.003–0.860	TG	14

Experimental

Measurement method

The TG–DTA measurements were made with a Rapid Heating Rigaku Thermoflex TG–DTA unit. Samples of 20, 10 and 2.5 mg were weighed accurately in a platinum crucible (d 5.0 × h 2.5 mm), distributed evenly with a pin when a small amount was used, and tapped 2 or 3 times on a metal surface. An equal amount of "dead-burnt" α-alumina was used as the standard reference material. The control of Po_2 by mixing N_2, air and O_2, its monitoring by the EMF method [15], the characterization of the samples and the reaction products, and other experimental procedures, were performed in the same way as reported previously [16, 17].

Sample preparation

MoS_2: Highly pure MoS_2 (Wako Pure Chem. Inds. Ltd., 99.99%) was dried under vacuum at 150° for 12 h and sieved into grades for use as powder samples. The composition was determined to be $MoS_{2.000}$ by oxidizing the sample in air to

MoO_3. A single-crystal of molybdenite (collected from Hirase mine, Gifu Pref.) was cut into pieces (about 1 mg) and used as sample.

"Mo_2S_3": Since "Mo_2S_3" has a very narrow homogeneity range and its composition has been reported to be $MoS_{1.457}$ [3], highly pure molybdenum powder (Soekawa Chem. Inds. Ltd., 99.9%) and sulfur powder (Yoneyama Chem. Inds. Ltd., 99.5%) were mixed in this compositional ratio. The mixture was ground in acetone, dried under vacuum for 12 h, sealed in an evacuated quartz tube and heated at 400° for 2 days. The sample was then heated at 950° for 10 days before quenching in ice-water. Thus, the nominal nonstoichiometric composition of the "Mo_2S_3" used in this study was $MoS_{1.457}$. Neither any impurity phases nor any unreacted ingredients were found in the X-ray powder diffraction pattern (CuK_α) of the prepared sample.

Results and discussion

Thermal analysis of the oxidation of MoS_2

The TG–DTA curves for the oxidation of MoS_2 powder and the single-crystal in O_2 and in air at a heating rate of 10 deg min^{-1} are shown in Fig. 1. TG curves, both

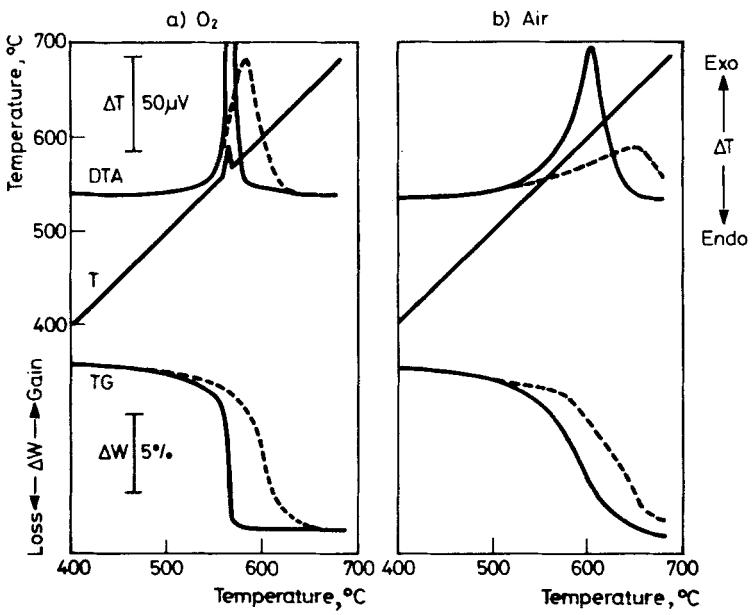

Fig. 1 TG–DTA curves for MoS_2 powder —— and single ..... crystal when heating at 10 deg min^{-1} in air and in O_2 (sample size: 10 mg; 250–270 mesh, gas flow: 2 ml s^{-1})

in O_2 and in air, show a single weight loss step, with a corresponding exotherm in the DTA curves. In air, a very slow weight loss started at around 450° and 560° for the powder and the single-crystal, respectively, and this weight loss became prominent at around 530° for the powder and 620° for the single-crystal. In O_2, an abrupt rise in sample temperature, together with a sudden loss of weight, was detected for the powder sample, but the reactions were much less violent in comparison with those of vanadium, titanium and niobium sulfides [16–19]. The sample temperature ceased to rise when Po_2 was set below 0.70 atm (Fig. 2). The X-

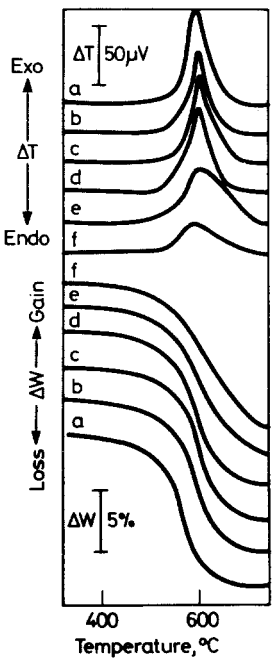

Fig. 2 TG–DTA curves for MoS_2 powder when heating at 10 deg min^{-1} in different P_{O_2} (sample size: 10 mg; 250–270 mesh, gas flow: 2 ml s^{-1}). *a:* 0.672 atm, *b:* 0.408 atm, *c:* 0.260 atm, *d:* 0.209 atm, *e:* 0.129 atm, *f:* 0.089 atm

ray diffraction patterns of the samples at the end of heating showed only MoO_3 orthorhombic peaks. The powder sample was heated separately at temperatures between 450 and 470° for 90 minutes, and the phases present after heating were checked by X-ray analysis. However, in contrast with the result of Ong [5], only orthorhombic MoO_3 and unreacted MoS_2 peaks were observed, instead of MoO_2. As the MoO_3 obtained by oxidizing the MoS_2 single-crystal preferred the orthorhombic *b*-axis direction, which corresponds to the hexagonal *c*-axis direction for the MoS_2 single-crystal, it can be concluded that the stacking property of the

oxide phase is similar to that of the mother MoS_2 single-crystal. This feature was not observed for the powder sample. For the powder sample, the agreement between the calculated 10.07% and observed 10.12% weight losses is good, if some additional loss of weight due to evaporation is considered [20]. However, when the single-crystal was used, the reaction started at higher temperature and a substantial amount of MoO_3 was sublimed before the completion of oxidation.

On the basis of the above analysis, the oxidation process of MoS_2 powder or single-crystal can be described by Eq. (1). Our results agree with those of Wilkomirsky et al. [10], Doheim et al. [11] and Ross et al. [12], but differ from others [5–9] in that MoO_2 is formed before the beginning of MoO_3 formation.

The same oxidation process was observed irrespective of Po_2 (1–0.0890 atm) and the heating rate (2–20 deg min^{-1}). The TG–DTA curves for MoS_2 powder obtained at different Po_2 and at a heating rate of 10 deg min^{-1} are shown in Fig. 2. Under these conditions, there was no rise in sample temperature due to the heat of reaction, and there was no side-reaction either. It is clear from the above findings that a kinetics study according to Eq. (1) is possible if powder sample is used.

Kinetic study on the oxidaton of MoS_2 powder

A kinetic study on the oxidation of MoS_2 powder is possible, since MoS_2 powder is oxidized to MoO_3 in a single step, without any rise in sample temperature, over the whole Po_2 range studied (0.612–0.089 atm).

Isothermal method

α vs. t plot

The samples were oxidized isothermally between 540 and 625°, selected from the nonisothermal analysis. A blank experiment, with an equal amount of α-alumina instead of sample, was performed at each temperature to correct for the drift of the TG pen during the instantaneous rise in furnace temperature. The corrected TG traces were then used to calculate the fraction reacted at a difinite time t. Typical plots of α *vs.* t are shown in Fig. 3.

Rate equation

The most appropriate rate equation is considered to be the one which gives the best line fit when plotted against time. All possible rate equations were tested by using a computer program [17]. Plots obtained for different conditions (e.g. temperature, Po_2, particle size etc.) were examined carefully to select the most appropriate rate equation. This examination showed that the reaction represented by Eq. (2) conformed to the rate equation

$$1-(1-\alpha)^{1/3} = kt \qquad (2)$$

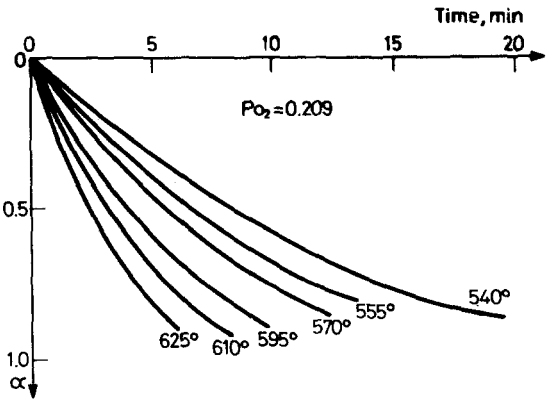

Fig. 3 Typical α *vs.* t plots for MoS_2 powder (sample size: 2.5 mg; 250–270 mesh, gas flow: 2 ml s^{-1})

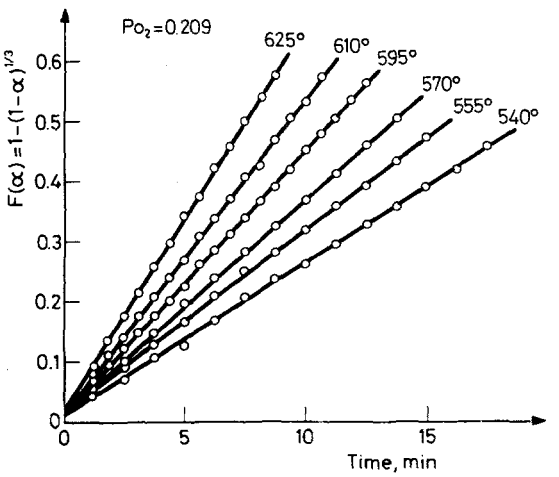

Fig. 4 Plots of rate equation $[F(\alpha) = 1-(1-\alpha)^{1/3}]$ *vs.* t (sample size: 2.5 mg; 250–270 mesh, gas flow: 2 ml s^{-1})

as shown in Fig. 4. This equation corresponds to a three-dimensional phase boundary reaction or a shrinking core model, indicating that a sphere react from all surfaces of the particle inwards.

Dependence of E and A on Po_2

Arrhenius plots for different Po_2 are shown in Fig. 5, and the apparent activation energy E and pre-exponential factor A obtained from the plots are listed in Table 2. It can be seen that the Arrhenius plots are parallel to one another and E is stable if a high enough Po_2 ($0.129 \leqq Po_2 \leqq 0.612$) is available in the reaction chamber for

oxidation [18, 19]. The value of E (98.1 ± 2.2 kJ mol^{-1}) determined under the present experimental conditions is reasonably close to the result of Doheim et al. [11], but differs considerably from others (Table 1). However, direct comparison of the results is not possible, since we used pure MoS_2 instead of the molybdenite concentrate used by others.

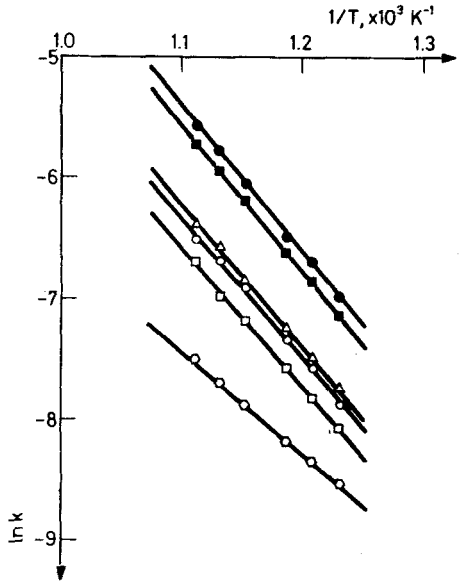

Fig. 5 Arrhenius plots for MoS_2 powder in different P_{O_2} (sample size: 2.5 mg; 250–270 mesh, gas flow: 2 ml s^{-1}). P_{O_2} values: ● 0.612, ■ 0.408, △ 0.260, ○ 0.209, □ 0.129, ○ 0.0890

Table 2 Apparent activation energy and pre-exponential factor for oxidation of MoS_2 powder at different P_{O_2} (sample size: 2.5 mg, 250–270 mesh)

P_{O_2}, atm	Isothermal method		Nonisothermal method (10 deg min^{-1})
	E, kJ mol^{-1}	A, 1/s	E, kJ mol^{-1}
0.612	101	2.50×10^3	97.4
0.408	100	2.14×10^3	95.3
0.260	96.8	717	93.6
0.209	96.2	600	91.0
0.129	96.4	483	90.0
0.089	70.3	6.33	80.0

$1-(1-\alpha)^{1/3} = kt$.

Dependence of k on Po_2 and particle size

Figure 6 shows the plots of $-\log k$ vs. $-\log Po_2$ (Po_2 = 0.612–0.0890 atm). It is seen that the plots are almost parallel at each temperature for the Po_2 where E is stable. At the lowest Po_2 (0.0890 atm), where E decreases greatly, k also decreases abruptly. From these plots, the relationsip between k and Po_2 was determined as

$$k = c' \cdot (Po_2{}^{0.491 \pm 0.034}) \tag{3}$$

for the temperature range 540–570°.

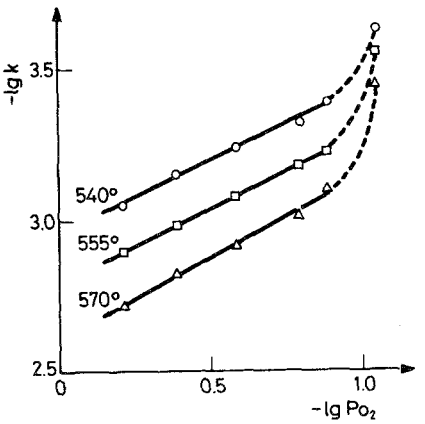

Fig. 6 Plots of $-\log k$ *vs.* $-\log P_{O_2}$ for MoS_2 powder (sample size: 2.5 mg; 250–270 mesh, gas flow: 2 ml s^{-1})

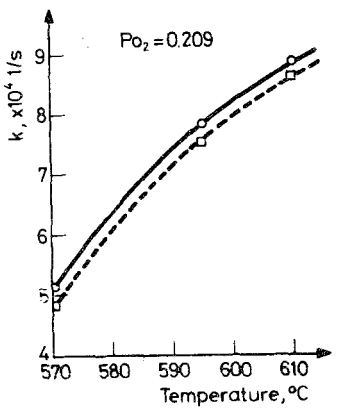

Fig. 7 Variation of k with particle size (sample size: 2.5 mg, gas flow: 2 ml s^{-1}, ○ 250–270 mesh, □ 100–150 mesh)

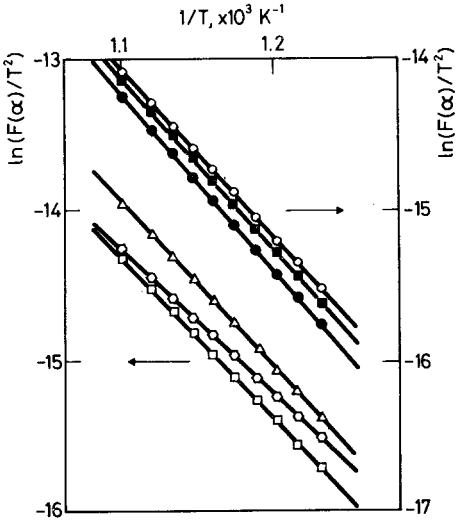

Fig. 8 Coats and Redfern linearization plots for MoS_2 powder in different P_{O_2} (heating rate: 10 deg min^{-1}; sample size: 2.5 mg; 250–270 mesh, gas flow: 2 ml s^{-1}). P_{O_2} values: ● 0.612, ■ 0.408, ○ 0.260, △ 0.209, □ 0.129, ○ 0.0890

The rate constants were determined for 250–270 and 150–200 mesh samples. Figure 7 shows that the value of k with respect to temperature decreased very slightly with increase of the particle size. As Amman et al. [13] indicated, this result lends support to the shrinking core kinetic model.

Nonisothermal method

The Coats and Redfern method [21] was used for the nonisothermal study. Typical plots are shown in Fig. 8, and the results for E obtained in the same Po_2 range as applied for the isothermal study are listed in Table 2. The good agreement between the values obtained with this and the isothermal methods undoubtedly proves the accuracy of the rate equation determined with the isothermal method [19].

Thermal analysis of the oxidation of "Mo_2S_3"

The TG–DTA curves for the oxidation of "Mo_2S_3" in air and in oxygen at a heating rate of 10 deg min^{-1} are shown in Fig. 9. The DTA curves exhibit four exothermic peaks, whereas the TG curves show only two steps of weight change, corresponding to peaks III and IV in the DTA curves. Unlike the oxidation of vanadium sulfides [16], the profiles of these curves remain unchanged at different

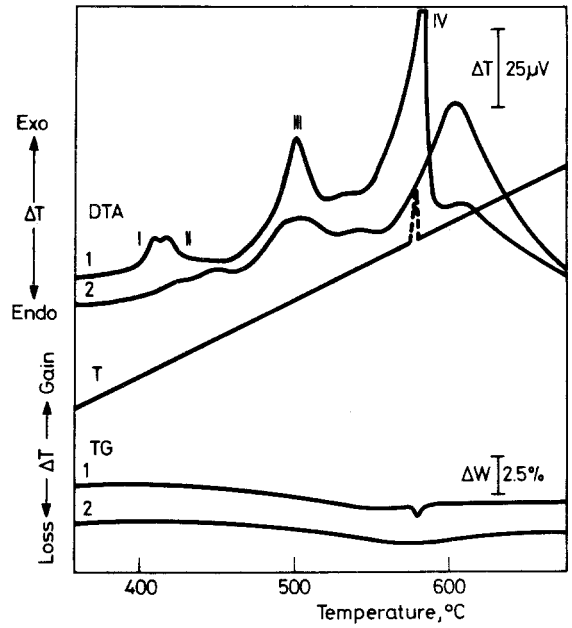

Fig. 9 TG–DTA curves for "Mo_2S_3" when heating at 10 deg min^{-1} in O_2 – – – and in air —— (sample size: 10 mg; 250–270 mesh, gas flow: 2 ml s^{-1})

Table 3 Onset, peak and end temperatures and weight change in each DTA peak (10 deg min^{-1})

Atmosphere	Peak no.	Temperature, °C			Weight change, %
		onset	peak	end	
O_2 flow	I	402	415	420	—
	II	422	424	430	—
	III	456	505	522	−2.5
	IV	548	*	598	+0.8
				total	−1.7
air flow	I	392	425	430	—
	II	430	447	452	—
	III	452	503	538	−2.3
	IV	538	604	653	+1.1
					−2.2

* : Measurement is impossible because of the rise in sample temperature.

heating rates (2–20 deg min^{-1}). The temperature of each DTA peak and the weight change in each TG step are listed in Table 3. The samples were quenched at the end of each DTA peak, and the products were identified by X-ray analysis. It is evident from this analysis that the oxidation proceeds as follows:

(i) surface oxidation of the sample to γ-Mo_4O_{11},
(ii) formation of MoO_2,
(iii) oxidation of unreacted "Mo_2S_3" to MoO_2, and
(iv) oxidation of MoO_2 to MoO_3.

(i) Surface oxidation of the sample to γ-Mo_4O_{11}

X-ray analysis of the sample at the end of the 1st DTA peak showed the presence of a very slight amount of monoclinic Mo_4O_{11} phase (γ-Mo_4O_{11}). The intensity of the powder diffraction pattern did not change and the TG curve did not record any weight change, even when the sample was heated constantly at the peak temperature. It is presumed from this fact that the surface of the sample is oxidized rapidly to γ-Mo_4O_{11}, according to Eq. (4), and that once the surface is covered with the oxide, the reaction automatically ceases to proceed:

$$\text{"}Mo_2S_3\text{"}_{(sur)} + 23/4\,O_2 \rightarrow 1/2\,\gamma\text{-}Mo_4O_{11(sur)} + 3\,SO_2 \qquad (4)$$

where subscript '(sur)' indicates the surface layer.

(ii) Formation of MoO_2

Instead of γ-Mo_4O_{11} peaks, MoO_2 peaks appeared in the diffraction pattern of the sample quenched at the end of the 2nd DTA peak. As in step (i), the curve did not show any weight change, and the intensity of the MoO_2 peaks in the diffraction pattern did not increase during heating at the peak temperature. This fact suggests that in this stage γ-Mo_4O_{11} reacts with "Mo_2S_3" and O_2 to form MoO_2, according to the reaction

$$\gamma\text{-}Mo_4O_{11(sur)} + \text{"}Mo_2S_3\text{"} + 7/2\,O_2 \rightarrow 6\,MoO_{2(sur)} + 3\,SO_2 \qquad (5)$$

This reaction comes to an end when the surface γ-Mo_4O_{11} layer is consumed.

(iii) Oxidation of the residual "Mo_2S_3" to MoO_2 and
(iv) Oxidation of MoO_2 to MoO_3

The unreacted "Mo_2S_3" was oxidized directly to MoO_2 in peak III, and MoO_2 in turn was oxidized to MoO_3 in peak IV. The reactions for these steps are

$$\text{unreacted "}Mo_2S_3\text{"} + 5\,O_2 \rightarrow 2\,MoO_2 + 3\,SO_2 \qquad (6)$$

$$MoO_2 + 1/2\,O_2 \rightarrow MoO_3 \qquad (7)$$

However, the weight changes corresponding to peaks III and IV overlapped in the TG curves. Consequently, the observed weight change for these steps are much less than the calculated values (-10.32% and $+11.22\%$ for peaks III and IV respectively). Further the final weight change observed when the sample was oxidized in oxygen (-1.7%) or in air (-2.2%) did not agree with the calculated value ($+0.90\%$). This disagreement is due to the evaporation of MoO_3 formed in step (iv).

Conclusions

1. MoS_2 powder and single-crystal are oxidized directly to MoO_3:

$$MoS_2 + 7/2\,O_2 \rightarrow MoO_3 + 2\,SO_2$$

For MoS_2 powder, the process is controlled by a three-dimensional phase boundary reaction:

$$1-(1-\alpha)^{1/3} = kt$$

where $\alpha = 0.01$–0.90.

The values of E determined with the isothermal and the nonisothermal methods (10 deg min^{-1}) are 98.1 ± 2.2 and 93.5 ± 3.0 kJ mol^{-1}, respectively, over the Po_2 range 0.612–0.0890 atm and the temperature range 540–625°. The relationship between k and Po_2 is

$$k = c' \cdot (Po_2)^{0.491 \pm 0.034}$$

where $Po_2 = 0.612$–0.129 atm.

2. The principal oxidation processes of "Mo_2S_3" in air and in O_2 flows (2 ml s^{-1}) are as follows

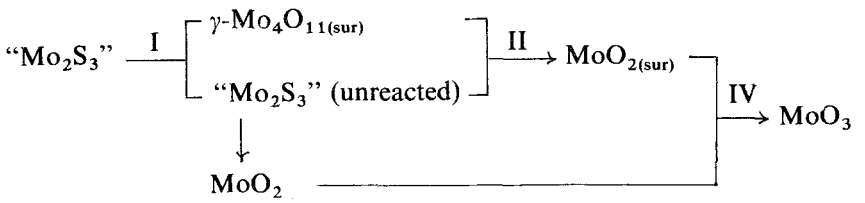

The above processes are valid for a wide range of heating rates (2–20 deg min^{-1}).

* * *

We thank Sumiko Lubricant Co. Ltd. for supplying the single-crystals of MoS_2 used in the above experiments.

References

1 G. H. Moh, Gh. Udubasa and R. Hüller, Metall, 28 (1974) 804.
2 H. Rau, J. Phys. Chem. Solids, 41 (1980) 765.
3 Y. Suzuki, T. Uchida, M. Wakihara and M. Taniguchi, Mat. Res. Bull., 16 (1981) 1085.
4 W. E. Jamison and S. L. Cosgrove, ASLE Trans., 14 (1971) 62.
5 J. N. Ong, University of Utah, Ph.D. Thesis, 1955.
6 A. N. Zelikman and L. V. Belaevskaya, J. Inorg. Chem. USSR, 10 (1956) 2245.
7 I. Galateanu, Rev. Chim. Bucharest, 8 (1957) 363.
8 I. Galateanu, Ibid., 7 (1956) 531.
9 L. Condurier, I. A. Wilkomirsky and G. Morizot, Trans. Inst. Min. and Metall., Sect. C, 79 (1970) C34.
10 I. A. Wilkomirsky, A. P. Watkinson and J. K. Brimacombe, Ibid, 84 (1975) C197.
11 M. A. Doheim, M. Z. Abdel-Wahab and S. A. Rassoul, Met. Trans. B, 7B (1976) 477.
12 S. Ross and A. Sussman, J. Phys. Chem., 59 (1955) 889.
13 P. R. Amman and T. A. Loose, Met. Trans., 2 (1971) 889.
14 C. Cardoen, University of Utah, Ph.D. Thesis, June 1969.
15 T. H. Etsell and S. N. Flengas, Metall. Trans., 3 (1972) 27.
16 S. K. Basu and M. Taniguchi, J. Thermal Anal., 29 (1984) 1209.
17 S. K. Basu and M. Taniguchi, Ibid, 30 (1985) 1129.
18 S. K. Basu and M. Tanigushi, Thermochim. Acta, 109 (1986) 253.
19 S. K. Basu and M. Taniguchi, Ibid, to be published.
20 G. Ramadorai, M. E. Wadsworth and C. K. Hansen, Metall. Trans. B, 6B (1975) 579.
21 A. W. Coats and J. P. Redfern, Nature, 201 (1964) 68.

Zusammenfassung — Mittels TG- und DTA-Methoden wurden im P_{O_2}-Bereich 1 bis 0,0890 atm thermische Oxydationsvorgänge an stöchiometrischem MoS_2 und nichtstöchiometrischem „Mo_2S_3" sowie die Kinetik der Oxydation von MoS_2 untersucht. MoS_2 wird in einem Schritt vollständig zu MoO_3 oxydiert:

$$MoS_2 + 7/2\,O_2 \rightarrow MoO_3 + 2\,SO_2$$

Unabhängig von P_{O_2} und der Aufheizgeschwindigkeit wird „Mo_2S_3" über die folgenden vier Schritte zu MoO_3 oxydiert:

$$\text{„}Mo_2S_3\text{"} \xrightarrow{\text{I}} \gamma\text{-}Mo_4O_{11(sur)} + \text{„}Mo_2S_3\text{"} \xrightarrow{\text{II}}$$

$$MoO_{2(sur)} + \text{„}Mo_2S_3\text{"} \xrightarrow{\text{III}} MoO_2 \xrightarrow{\text{IV}} MoO_3$$

wobei sich (sur) auf die Oberflächenschicht bezieht. Laut kinetischer Untersuchungen läuft die Oxydation (α = 0.01–0.90) von MoS_2 zu MoO_3 nach der Gleichung $1-(1-\alpha)^{1/3} = kt$ ab; die durch isotherme bzw. nichtisotherme (10 grd/min) Methoden bestimmten virtuellen Aktivierungsenergien betragen 98.1 ± 2.2 bzw. 93.5 ± 3.0 kJ/mol im Temperaturbereich 540–625 °C und in einem P_{O_2}-Bereich von 0.612–0.129 atm. Die Beziehung zwischen der Geschwindigkeitskonstante k und P_{O_2} wurde ermittelt.

Резюме — Методами ТГ и ДТА в атмосфере кислорода с P_{O_2} 1–0,0890 атм изучены процессы термического окисления стехиометрического MoS_2 и нестехиометрического «Mo_2S_3», наряду с кинетикой окисления дисульфида молибдена. MoS_2 окисляется до MoO_3 в одну стадию:

$$MoS_2 + 7/2\,O_2 \rightarrow MoO_3 + 2\,SO_2$$

Нестехиометрический «Mo_2S_3», независимо от давления кислорода и скорости нагрева, окисляется до конечного MoO_3 в четыре стадии:

$$\text{«}Mo_2S_3\text{»} \xrightarrow{\text{I}} \gamma\text{-}Mo_4O_{11(\text{пов.})} + \text{«}Mo_2S_3\text{»} \xrightarrow{\text{II}}$$

$$MoO_{2(\text{пов.})} + \text{«}Mo_2S_3\text{»} \xrightarrow{\text{III}} MoO_2 \xrightarrow{\text{IV}} MoO_3,$$

где пов. обозначает поверхностный слой. Изучение кинетики показало, что окисление дисульфида молибдена до трехокиси молибдена (α = 0.01–0.90) подчинается кинетическому уравнению $1-(1-\alpha)^{1/3} = kt$. Кажущиеся энергии активации, определенные изотермическим и неизотермическим методом (0 град·мин$^{-1}$), равнялись, соответственно, 98.1 ± 2.2 и 93.5 ± 3.0 кдж·моль$^{-1}$ в области температур 540–625° и давлении кислорода 0.612–0.129 атм. Установлена взаимосвязь между константой скорости k и P_{O_2}.